

Synthesis of Magnetite/Amphiphilic Polymer Composite Nanoparticles as Potential Theragnostic Agents

James Wainaina¹, Na Hae Kim¹, Juyoung Kim^{1,*}, Moonsoo Jin², and Soo Haeng Park³

¹Department of Advanced Materials Engineering, Kangwon National University,
Samcheok City, Kangwon-Do 245-711, South Korea

²Department of Biomedical Engineering, Cornell University, Ithaca, NY 14850, USA

³School of General Studies, Kangwon National University, Samcheok City, Kangwon-Do 245-711, South Korea

This study describes the synthesis of magnetite/amphiphilic polymer composite nanoparticles that can be potentially used simultaneously for cancer diagnosis and therapy. The synthesis method was a one-shot process wherein magnetite nanoparticles were mixed with core-crosslinked amphiphilic polymer (CCAP) nanoparticles, prepared using a copolymer of a urethane acrylate nonionomer (UAN) and a urethane acrylate anionomer (UAA). The CCAP nanoparticles had a hydrophobic core and a hydrophilic exterior with both PEG segments and carboxylic acid groups, wherein the magnetite nanoparticles were coordinated and stabilized. According to DLS data, the ratio of UAN to UAA and the ratio of magnetite to polymer are keys to controlling the size and thus, the stability of the composite nanoparticles. The magnetic measurement indicated that the composite nanoparticles had superparamagnetic properties and high saturation magnetization. The preliminary magnetic resonance imaging showed that the particles produced an enhanced image even when their concentration was as low as 80 $\mu\text{g/ml}$.

Keywords: Polymer, Magnetite, Amphiphilic, Nanoparticles, Composite, MRI.

1. INTRODUCTION

Due to the unique magnetic property (superparamagnetic property) of magnetic nanoparticles, they have been widely used in electronics, biotechnology, and environmental technology. Especially, colloidal dispersion of magnetite nanoparticles or magnetic fluids that contain magnetite nanoparticles stabilized by surfactants or polymers have shown highly promising applications in bio-separation, drug delivery vehicles, MRI contrast agents, and high-gradient magnetic separation.^{1–6} For these applications, the magnetic nanoparticles should have high water dispersibility, biocompatibility, high magnetic susceptibility, and a long residence time in the body, and should be capable of being easily and completely separated by exterior magnetic fields.

Magnetite nanoparticles can easily have high water dispersibility, biocompatibility, and a long residence time in the body if their surface is coated with hydrophilic polymers. In most cases, hydrophilic polymers with carboxylic acid groups are chemisorbed onto the magnetic surface and provide electrostatic stabilization.^{7–8} Electrostatically

stabilized magnetite nanoparticles could be easily aggregated, however, by changing the pH of the colloidal medium. To improve the colloidal stability of these nanoparticles, surfactants or amphiphilic polymers with non-ionic hydrophilic groups, such as polyethylene oxide (PEO)-polypropylene oxide (PPO) block copolymers, are frequently and widely used as co-stabilizers. Additionally, amphiphilic polymers with PEO or polyethylene glycol (PEG) segments can significantly reduce the adsorption of proteins or blood platelets onto magnetic nanoparticles and their uptake by macrophages, which can prolong their circulation time in the body and enhance their permeability and retention (EPR) effect.⁹

Polymeric layer coating on magnetic nanoparticles can give the nanoparticles colloidal stability and biocompatibility but significantly reduces their magnetic susceptibility. In most cases, magnetite nanoparticles stabilized by polymers have a core/shell microstructure wherein the magnetite nanoparticles are located at the core and the polymers are located on the outer layer. As the thickness of the outer polymer increases, the colloidal stability, biocompatibility, circulation time, EPR effect, and payload of the drug increase but its magnetization and magnetic susceptibility decrease or vice versa.¹⁰ As a result, it has been

*Author to whom correspondence should be addressed.

most difficult to prepare magnetite/polymer composite nanoparticles with high colloidal stability and biocompatibility without sacrificing their magnetic properties.

This study was conducted to present a new process for the preparation of novel magnetite/amphiphilic polymer composite nanoparticles. Unlike the conventional magnetite/polymer composite nanoparticles with a core-shell nanostructure, the composite nanoparticles in this study were prepared using core-crosslinked amphiphilic polymer (CCAP) nanoparticles dispersed in water as nanotemplates wherein the magnetite nanoparticles were located and stabilized via electrostatic and steric stabilization. According to the authors' preceding paper, CCAP nanoparticles synthesized with urethane acrylate nonionomers had a cross-linked hydrophobic core and a hydrophilic outer shell. These nanoparticles encapsulated cancer drugs and showed excellent target delivery performance without any toxicity in normal cells.¹¹ Thus, magnetite/CCAP composite nanoparticles can be expected to simultaneously aid in MRI image enhancement and satisfactory target drug delivery performance.

This paper will first present the preparation of nanoclusters that consisted of magnetite nanoparticles and CCAP

nanoparticles through the nanoprecipitation process. The change in the size and colloidal stability of these nanoclusters was monitored at various UAN and UAA chain compositions to explore the optimal composition of magnetic nanoclusters with higher colloidal stability and with the highest magnetite content. The morphology of the synthesized nanoclusters, measured via TEM, will also be presented to discuss their microstructures.

2. EXPERIMENT DETAILS

2.1. Synthesis of Poly(UAN-UAA) Solutions

The urethane acrylate nonionomer (UAN) and urethane acrylate anionomer (UAA) that were used in this study were synthesized using the previously published procedures in¹² and,¹³ respectively. The molecular structure of UAN is schematically shown in Figure 1(a), and that of UAA is shown in Figure 1(b).

To prepare the poly(UAN-UAA) solutions, UAN and UAA, at various weight ratios, were dissolved in dimethylacetamide (DMAC) and transferred to a 100 ml three-necked round-bottom flask equipped with a magnetic

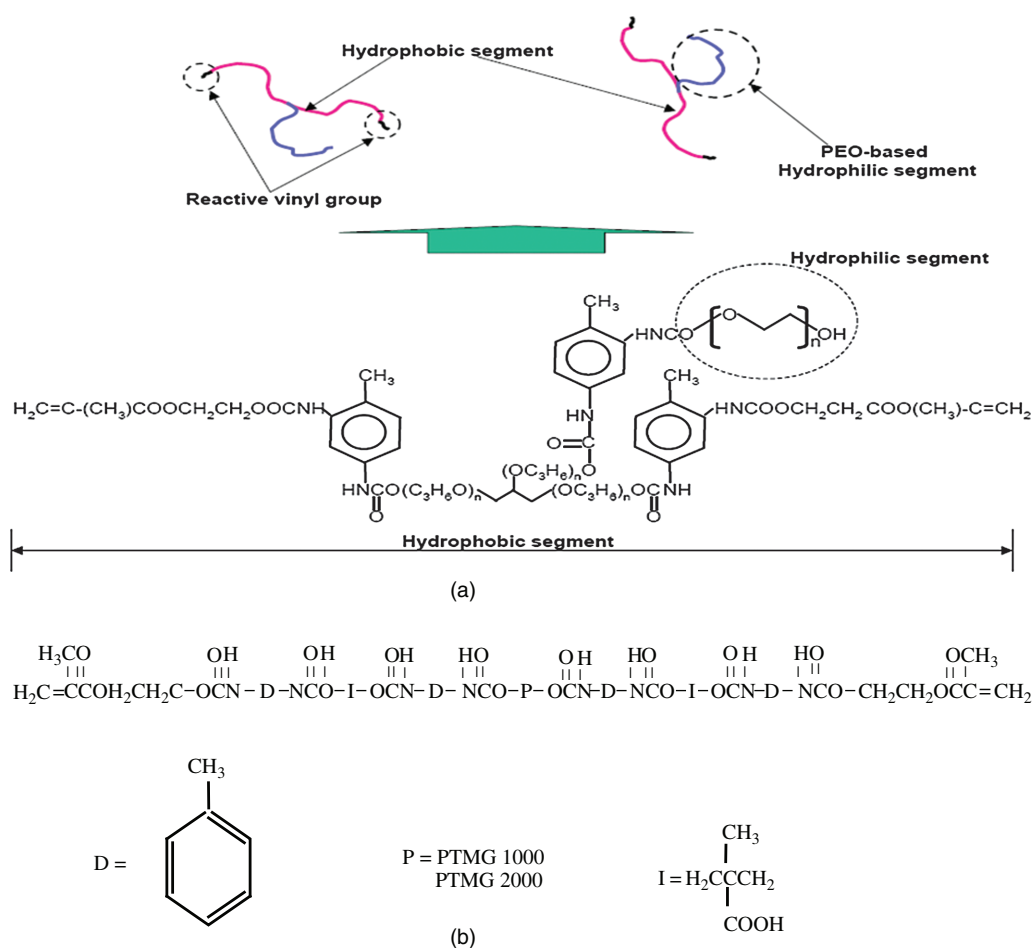


Fig. 1. Schematic of (a) the UAN molecular structure and (b) the UAA molecular structure.

stirrer, thermometer, nitrogen inlet, and oil heating system. Then the temperature was raised to 80 °C, and polymerization was allowed to continue for 6 h with constant stirring and in the presence of azobisisobutyronitrile (AIBN) as an initiator.

2.2. Synthesis of the Magnetite Nanoparticles

The magnetite nanoparticles (2–15 nm) were synthesized using the co-precipitation method,^{14–16} wherein 0.368 g of iron II chloride tetrahydrate and 1 g of iron III chloride hexahydrate were dissolved in 20 g of water and poured into a three-necked kettle equipped with a mechanical stirrer and an inlet system for nitrogen gas. To deoxygenate the solution, the solution was purged of nitrogen for 30 min before it was co-precipitated and maintained throughout the experiment. The co-precipitation was carried out at room temperature with the addition of concentrated sodium hydroxide with vigorous stirring. The formation of a dark precipitate was immediately observed upon the addition of the sodium hydroxide solution.

2.3. Synthesis of Magnetite/Poly(UAN-UAA) and NTA Conjugated Composite Nanoparticles

0.9 g of magnetite nanoparticles was suspended in 5.0 ml of water in a 50 ml beaker and homogenized via ultrasonication for 20 min. Then 0.3 g of the poly(UAN-UAA)-DMAC solution was added dropwise and mixed with vigorous stirring for 12 h. The prepared mixtures were dropped into 50 mL of DDI water to prepare composite nanoparticles dispersed in an aqueous phase. The colloidal solution was centrifuged and washed five times with distilled water to separate the aggregated magnetite particles.

To prepare nitrilotriacetic acid (NTA)-functionalized composite nanoparticles, $N\alpha$ $N\alpha$ -bis(carboxymethyl)-L-lysine hydrate (NTA analog) was first grafted on the PEG chains of the CCAP nanoparticles, according to a previously published two-step procedure.¹¹ Then the NTA-functionalized CCAP nanoparticles were mixed with the magnetite nanoparticles according to the aforementioned procedure.

2.4. *In Vitro* MR Imaging

The MR image enhancement capability of the magnetite/poly(UAN-UAA) composite nanoparticles was assessed by conducting an *in vitro* experiment on a 3 T Signa (GE) Clinical Scanner. The MRI phantom was prepared by mixing 100 μ l of the composite nanoparticles with 100 μ l of agarose before adding the mixture to a 1.5% agarose gel in a 60 ml centrifuge tube.

3. RESULTS AND DISCUSSION

When poly(UAN-UAA) chains are mixed with water, they are self-assembled to form core-crosslinked amphiphilic polymer (CCAP) nanoparticles via hydrophilic/hydrophobic nanophase separation. That is, the hydrophobic PPO segments of the poly(UAN-UAA) chains are associated with each other to form a chemically cross-linked hydrophobic core, whereas the hydrophilic PEG segment and the carboxylic segments are oriented to the aqueous phase to form a hydrophilic outer layer. Due to this nanostructure, CCAP nanoparticles could payload water-insoluble drugs within their hydrophobic interior and disperse them as nanoparticles in water. When the CCAP nanoparticles come in contact with the magnetite nanoparticles, the carboxylic groups of the CCAP nanoparticles can be expected to coordinate the iron atoms on the surface of the magnetite nanoparticles at the same time, and the hydrophilic PEG chains can be expected to form a magnetite nanoparticle-CCAP complex nanodispersed in water via steric stabilization.^{17–18}

3.1. Morphology and Particles Size

Considering the individual CCAP nanoparticles, the composite nanoparticles would be expected to adopt the red currant morphology proposed by Mayer.¹⁹ The TEM image in Figure 2(a), however, suggests the bridging of the individual composite nanoparticles to form a nanoclustered morphology with the magnetite nanoparticles (2–15 nm) concentrated around the surface of the CCAP nanoparticles. This observation is supported by DLS data (Tables I and II) that show that the size of the composite nanoparticles was several times bigger than that of the CCAP nanoparticles. As mentioned, CCAP nanoparticles bond magnetite through the interaction between the carboxylic groups and the iron atoms on the surface of the magnetite nanoparticles. Due to the large surface area of individual magnetite nanoparticles, however, they have numerous iron atoms on their surface that can serve as coordinating sites.⁷ Thus, two or more CCAP nanoparticles can be bridged by coordinating with a common magnetite nanoparticle to form a nanoclustered structure, as shown in Figure 2(b).

The UAN to UAA ratio was varied to examine its effect on the sizes of the nanoclusters. The DLS data (Table I) showed that the size change with the increase in the UAA component was insignificant when the polymer:magnetite ratio was 1:3. When the polymer:magnetite ratio was maintained at 3:1, however, the size increased dramatically from 277 nm to 2,042.5 nm, as the UAN:UAA ratio varied from 1:0.2 to 1:2. As the UAA fraction increased, so did the concentration of the carboxylic groups on the CCAP nanoparticles, which increased the chance of the CCAP nanoparticles that coordinated with the common magnetite

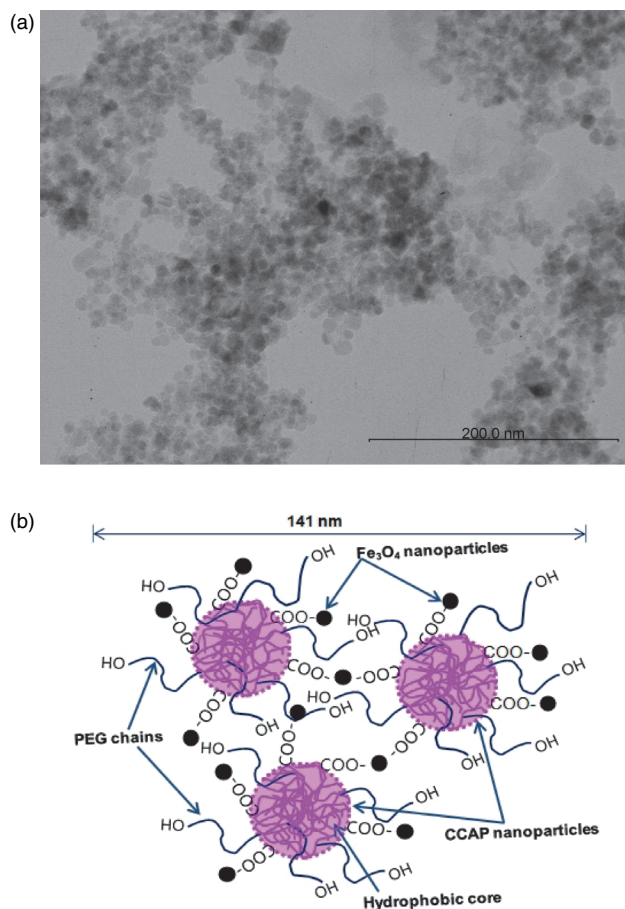


Fig. 2. (a) TEM image of the magnetite/poly(UAN-UAA) 1:0.4. (b) Schematic representation of the morphology of the particles.

nanoparticles to form clusters. At a low polymer concentration, however, the effect of the UAA was limited by the large interspacing distance between the individual CCAP nanoparticles. The clustering became more pronounced at a high polymer concentration due to the small interspacing distance between the CCAP particles, which made it easier for many particles to participate in the cluster formation.

3.2. Magnetite Content and Magnetic Properties

While the surface modification of magnetite improved its biomedical properties, the thick nonmagnetic coating

Table I. Particle sizes and magnetite content of magnetite/poly(UAN-UAA) composite nanoparticles at the ratio 1:3 (polymer:magnetite).

Sample	UAN:UAA (wt. ratio)	Particle Size (nm)		% Fe ₃ O ₄
		CCAP	Composite	
(a)	1:0.2	32	159.2	75
(b)	1:0.4	36	141.0	66
(c)	1:0.8	55	148.9	66
(d)	1:2	165	201.9	—

Table II. Particles sizes and magnetite content of magnetite/poly(UAN-UAA) composite nanoparticles at the ratio 3:1 (polymer:magnetite).

Sample	UAN:UAA (wt. ratio)	Particle Size (nm)		% Fe ₃ O ₄
		CCAP	Composite	
(a)	1:0.2	32	277.2	—
(b)	1:0.4	36	381.1	—
(c)	1:0.8	55	300.8	48
(d)	1:2	165	2042.5	—

often obtained in their core-shell structures greatly sacrifices their magnetization properties. This problem can be addressed by using two key features of CCAP nanoparticles:

(a) coordination of individual CCAP nanoparticles with multiple carboxylic groups with large numbers of magnetite nanoparticles, and

(b) coordination of the magnetite nanoparticles with the surface of the CCAP nanoparticles to reduce the nonmagnetic layer on the surface.

The magnetite content of the composite nanoparticles was assessed through a thermogravimetric analysis wherein the samples were heated from 25 °C to 950 °C in a nitrogen atmosphere, which allowed all the polymer components of the composite nanoparticles to decompose. The fraction that remained after the decomposition was attributed to the magnetite component. The results that are presented in Table I show that the magnetite proportion was high, which resulted in strong magnetization, as shown in Figure 3. The plots show that the saturation magnetization values of the magnetite/poly(UAN-UAA)

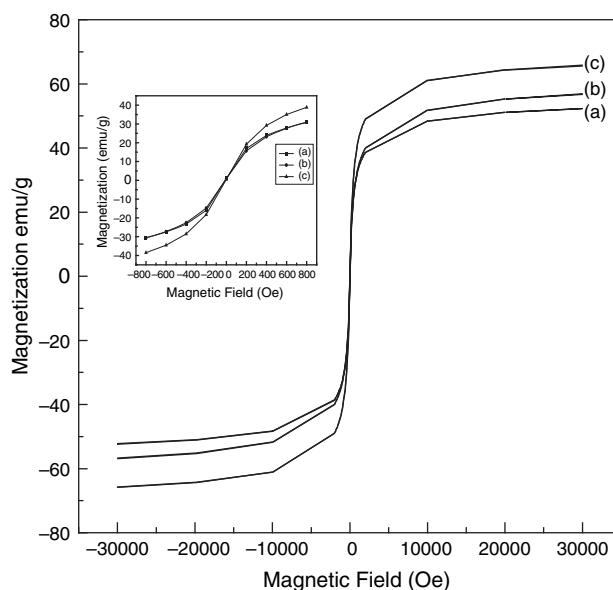


Fig. 3. Magnetization curves of the (a) magnetite nanoparticles, (b) magnetite/poly(UAN-UAA) 1:0.4, and (c) magnetite/poly(UAN-UAA) 1:0.8. Inset: plots for samples a, b, and c, between -800 and 800 Oe.

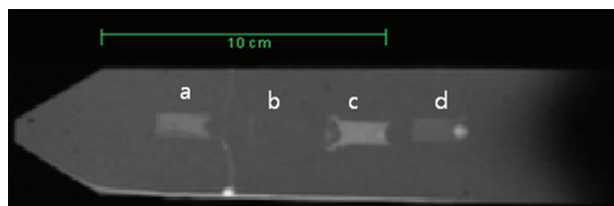


Fig. 4. MR image enhanced with (a) 462.5 $\mu\text{g/ml}$ of the NTA-functionalized composite particles at UAN : UAA = 1 : 2; (b) 46.25 $\mu\text{g/ml}$ of the NTA-functionalized composite particles at UAN : UAA = 1:2; (c) 800 $\mu\text{g/ml}$ of the unfunctionalized composite particles at UAN : UAA = 1 : 0.4; and (d) 80 $\mu\text{g/ml}$ of the unfunctionalized composite particles at UAN : UAA = 1 : 0.4.

composite nanoparticles at the UAN:UAA ratios of 1:0.4 and 1:0.8 were 56.75 emu/g and 65.74 emu/g, respectively. The values are even higher than that of the as-synthesized magnetite nanoparticles (52.23 emu/g). The particles were also found to have been superparamagnetic, as the plots showed no residual magnetism upon the removal of the magnetic field. This observation strongly indicates that CCAP nanoparticles do not compromise the magnetic properties of magnetite nanoparticles. The difference in the saturation magnetization values of the as-synthesized magnetite and the composite nanoparticles may be because bare magnetite nanoparticles are subject to oxidation during their storage, which may compromise their magnetic properties.²⁰

Figure 4 shows the T2 weighted MR images enhanced by the composite nanoparticles at various compositions. The figure shows that unmodified magnetite/poly(UAN-UAA) composite nanoparticles (1:0.4 UAN:UAA ratio) could produce an enhanced signal even at an 80 $\mu\text{g/ml}$ concentration, which highlights the potential of the particles as MR image enhancers. The relatively weaker signals produced by the NTA-functionalized composite nanoparticles was probably due to the increased number of organic components on the surface of the particles, and could be improved in the future by varying the amount of CCAP in the magnetite nanoparticles and controlling the NTA content on the surface of the particles.

4. CONCLUSIONS

Amphiphilic composite nanoparticles with potential theragnostic properties were prepared by mixing magnetite nanoparticles with core-crosslinked amphiphilic polymer (CCAP) nanoparticles. The exterior of the CCAP

nanoparticles had carboxylic groups to coordinate the magnetite nanoparticles, and PEG chains that provided stabilization via steric repulsion. The particles showed superparamagnetism and high saturation magnetization, which make them potentially powerful image enhancers, as shown by the MR image in Figure 4. The core of the CCAP nanoparticles was composed of hydrophobic PPO chains, and thus, they can act as nanocarriers for hydrophobic therapeutic agents.

Acknowledgment: This research (Grant No. 00042115) was supported by the Business for International Cooperative R&D between Industry, Academy, and Research Institute funded by the Korea Small and Medium-sized Business Administration in 2010.

References and Notes

1. J. L. Corhero and A. Villaverde, *Elsevier* 27, 268 (2009).
2. J. E. Smith, L. Wang, and W. Tan, *Trends in Analytical Chemistry* 25, 9 (2006).
3. S. Singh, *J. Nanosci. Nanotechnol.* 10, 7906 (2010).
4. H. W. Di, Y. L. Luo, F. Xu, Y. S. Chen, and Y. F. Nan, *J. Nanosci. Nanotechnol.* 10, 8210 (2010).
5. J. W. Moon, C. J. Rawn, A. J. Rondinone, W. Wang, H. Vali, L. W. Yeary, L. J. Love, M. J. Kirkham, B. Gu, and T. J. Phelps, *J. Nanosci. Nanotechnol.* 10, 8298 (2010).
6. S. Jiao, M. Xu, Y. Zhang, G. Pang, and S. Feng, *J. Nanosci. Nanotechnol.* 10, 8405 (2010).
7. M. Ming, Z. Yu, Y. Wei, S. Hao-Ying, Z. Hai-quian, and G. Ning, *Colloids and Surfaces A: Physicochem. Eng. Aspects* 212, 219 (2003).
8. Y. Zhang, N. Kohler, and M. Zhang, *Biomaterials* 23, 1553 (2002).
9. A. Aqil, S. Vasseur, E. Duguet, C. Passirani, J. P. Benoit, A. Roch, R. Muller, R. Jerome, and C. Jerome, *Eur. Polym. J.* 44, 3191 (2008).
10. Y. J. Chen, J. Tao, F. Xiong, J. B. Zhu, N. Gu, and K. K. Geng, *Pharmazie* 64, 481 (2010).
11. S. Park, S. Kang, A. J. Veach, Y. Vedvyas, R. Zarnegar, J. Y. Kim, and M. S. Jin, *Biomaterials* 31, 7766 (2010).
12. J. Y. Kim, H. M. Kim, D. H. Shin, and K. J. Ihn, *Macromonomer Chem. Phys.* 207, 925 (2006).
13. J. Y. Kim, Y. S. Chon, D. J. Yoo, and K. D. Suh, *J. Polym. Sci., Part B: Polym. Phys.* 38, 2081 (2000).
14. A. K. Gupta and M. Gupta, *Biomaterials* 26, 3995 (2005).
15. I. Nedkov, T. Merodiiska, L. Slavov, R. E. Vandenberghe, Y. Kusano, and J. Takada, *J. Magn. Magn. Mater.* 300, 358 (2006).
16. D. H. Kim, S. H. Lee, K. H. Im, K. N. Kim, K. M. Kim, I. B. Shim, M. H. Lee, and Y. K. Lee, *Current Applied Physics* 6S1, e242 (2006).
17. T. K. Jain, S. P. Foy, B. Erokwu, S. Dimitrijevic, C. A. Flask, and V. Labhasetwar, *Biomaterials* 30, 6748 (2009).
18. M. Klockenburg, J. Hilhorst, and B. H. Erne, *Vib. Spectrosc.* 43, 243 (2007).
19. A. B. R. Mayer, *Materials Science and Engineering* C6, 155 (1998).
20. R. L. Rebodos and P. J. Vikesland, *Langmuir* 26, 16745 (2010).

Received: 25 July 2011. Accepted: 11 January 2012.